Journal of Global Biosciences
ISSN 2320-1355
Volume 9, Number 2, 2020, pp. 6796-6806
Website: www.mutagens.co.in
DOI: www.mutagens.co.in/jgb/vol.09/02/090205.pdf

SCAN ME

Research Paper

OPTIMIZATION OF SILVER@SILICA NANOPARTICLES FOR BETTER ANTIMICROBIAL EFFICIENCY

Ameth Diagne[1], Bocar Noel Diop[2], Caroline Andreazza[3] and Mbacké Sembène[1]

[1]Département de Biologie Animale,
Faculté des sciences et Techniques, Université Cheikh Anta Diop (UCAD), Senegal ;
[2]bnd sciences, Senegal ;
[3]Interfaces, Confinement,
Matériaux et Nanostructures (ICMN) - UMR 7374 CNRS - Université d'Orléans,
France.

Abstract

Silver@silica hybrid nanoparticles have been identified as candidates of interest because metal cores have been highly biocidal towards microbes. The objective of this study was to optimize cost-effectiveness of these nanoparticles and to determine the most relevant parameters and mechanisms influencing antimicrobial activity. Silver@silica nanoparticles were synthesized by reverse microemulsion and their antimicrobial activity tested on *Aspergillus flavus*. Structural and morphological evolution of silver@silica nanoparticles was determined when silver concentration increased. Effect of ammonia and molar percentage of APTES relative to TEOS (% APTES) were also examined in order to be optimized in terms of cost. Results showed that antimicrobial efficacy of Silver@Silica nanoparticles increased as percentage of silver encapsulated in the silica matrix increased. However, beyond 10 mg/L of silver in the microemulsion, silver nanoparticles were no longer encapsulated in the silica matrix. Detailed examination of synthesis parameters that influence antimicrobial character of silver@silica nanoparticles allowed us to design an antimicrobial agent with an optimal cost/efficiency ratio with an oligodynamic character.

Key words: Silver@silica nanoparticles, optimization, antimicrobial, *Aspergillus flavus*.

INTRODUCTION

Metal products have attracted interest, particularly because of recent demonstrations of their strong antimicrobial character **[1]**. This type of product is generally used in care and biomedical devices at risk such as catheters, prostheses and dressings to reduce infections and prevent bacterial colonization. They are also used as an antimicrobial

agent in the treatment of water, in food packaging, various household appliances and as pesticides **[2]**. Among them, products containing silver in the form of nanometric particles have been very virulent towards microorganisms **[3]**. To get the full potential of their antimicrobial properties, however, it is necessary to protect these silver nanoparticles, and the proposed approach is to encapsulate them in an inert layer of silica.

Silver@silica hybrid nanoparticles have been identified as candidates of interest because metal cores have been highly biocidal towards different strains of bacteria and fungi **[4, 5]**. The advantage of this type of core@shell nanostructure is that silica layer makes it possible to ensure better chemical stability as well as better dispersion of silver nanoparticles **[6]**. In addition, silica layer simplifies the introduction to the surface of functional chemical groups that will allow the connection of the assembly to other materials, objects or macromolecules **[4]**. Encapsulation of silver nanoparticles in a nanoscale silica matrix also limits uncontrolled and rapid dissolution as would be the case for readily soluble silver salts, allowing long-acting antimicrobial action **[3]**. However, in order to define the efficient operating conditions of silver@silica nanoparticles, it seems to us absolutely necessary to optimize their efficiency and to provide elements of response to mechanisms for release of silver. A systematic study of silver/silica ratio coupled with a fine study of size and structure of elaborated nanoparticles must be performed to determine the role of each of these parameters on the antimicrobial effect.

The study focuses on the determination of structural, morphological and compositional evolution of silver@silica nanoparticles when silver/silica ratio varies and correlates these different parameters and response to antimicrobial tests. The aim was to optimize cost-effectiveness of these new nanomaterials and to determine the most relevant parameters and mechanisms that influence antimicrobial activity.

MATERIALS AND METHODS

Synthesis of silver@silica nanoparticles

Silver@silica type B4 nanoparticles are synthesized by inverse microemulsion according to the Diop protocol **[4]**. 3.5 ml of Triton X-100, 3.56 ml hexanol, 14.85 ml cyclohexane and 2.3 ml water were introduced at room temperature under stirring in a

30 ml bottle. Then, 14.6 mg silver nitrate solubilized in the aqueous phase of the microemulsion was reduced by 3 mg sodium borohydride in the presence of 0.101 ml aminopropyl triethoxysilale (APTES). After stirring for 30 minutes, 0.10 ml tetraethylorthosilicate (TEOS) and 0.06 ml ammonium hydroxide were added to the reaction medium to form the silica layer. The obtained mixture was left stirring overnight. Nanoparticles were separated from the reaction medium by addition of an equal volume of ethanol and centrifugation. With supernatant removed, nanoparticles were washed four times with ethanol.

Optimization of silver@silica nanoparticles

The main objective was to determine structural, morphological and compositional evolution of silver@silica nanoparticles when silver concentration increases. The effect of ammonia and the molar percentage of APTES relative to TEOS (% APTES) were also examined in order to be optimized in terms of cost.

Antimicrobial activity of silver@silica nanoparticles

Antimicrobial activity of silver@silica nanoparticles (B4, B6, B8 and B10) were evaluated on *Aspergillus flavus*. The technique consists of making a film of nanoparticles on surface of PDA culture medium. Variable amount of each type of silver@silica nanoparticles were deposited on surface of PDA. Each treatment replicated three times with controls (PDA without silver@silica nanoparticle). The efficiency of silver@silica nanoparticles treatment was evaluated after control competed by measuring the fungi colonies diameters. The Percent inhibition (PI) was calculated by using the following formula: $\mathrm{PI} = \frac{\mathrm{Da}-\mathrm{Db}}{\mathrm{Da}} \times 100$

Where Da is the diameter of mycelial growth in control medium and Db is the diameter of mycelial growth in medium treated by silver@silica nanoparticles.

Statistical analysis

Data were analysed using analysis of variance (ANOVA) and means were separated using Tukey-Kramer (HSD) test at $P < 0.05$, using R software version 3.5.3.

RESULTS

Silver@silica nanoparticles

The shape and size of silver@silica type B4 nanoparticles prepared in this study were checked by Transmission Electron Microscopy (TEM). Their structures under electron microscope are shown in **Figure 1** and their characteristics are shown in **Table 1**. The results showed that B4 nanoparticles were monodispersed with a well-defined core@shell structure.

Antimicrobial Activity of B4 nanoparticles

The results of antimicrobial tests of B4 nanoparticles against *Aspergillus flavus* were presented in **Table 2**. The growth of *A. flavus* was significantly reduced by B4 nanoparticles. The percent inhibition increased with concentrations. Between 2 and 30 mg the percent inhibition ranged from 16 % and 100 %.

Control of the amount of silver in silica matrix

The main technological lock when increasing the percentage of silver was to preserve the core@shell structure. Indeed, when the amount of silver of reaction medium was increased while keeping amounts of other constituents constant, we obtained non-encapsulated silver nanoparticles and empty silica nanoparticles (**Figure 2**).

Effect of mole percentage of APTES relative to TEOS (% APTES)

To improve encapsulation, we were interested in the APTES, reagent which serves to stabilize the silver nanoparticles while preparing their surface for growth of silica. **Figure 3** showed MET images of B8 nanoparticles obtained when molar percentage of APTES relative to the TEOS (% APTES) was increased beyond 20%.

TEM images of **Figure 3** showed that unencapsulated silver nanoparticles and empty silica nanoparticles were less numerous as %APTES increased. The exclusive obtaining of structures core@shell intervened from 35% of APTES, which corresponds to molar ratio APTES on Silver of approximately 5 as with nanoparticles B4. However, the increase in %APTES was accompanied by an increase in size and polydispersity of silver@silica nanoparticles, especially at 40%.

In view of these results the increase in the amount of silver must be accompanied by that of APTES in order to keep APTES ratio on silver equal 5. Thus silver@silica nanoparticles containing higher percentage of silver were synthesized with an APTES report on Silver equals 5 (**Figure 4**).

The amount of silver nanoparticles encapsulated in the silica matrix increased with mass concentration of Ag+ ions in the aqueous phase of the microemulsion. However, from 12g/L, good part of silver nanoparticles was not encapsulated. The amount of silver per silica ball therefore seems to be controllable by varying amount of solubilized silver in the reverse micelles with, however, a maximum of 10 g/L Ag in the aqueous phase of the microemulsion. The results obtained after size measurements and compositional characterizations were presented in **Table 3.**

Antimicrobial activity of B6, B8 and B10 nanoparticles

The results of antimicrobial tests of B6, B8 and B10 nanoparticles on Aspergillus flavus were presented in **Table 4**. B6, B8 and B10 nanoparticles strongly reduced the mycelial growth of *A. flavus* after 7 days of incubation at 32 °C. For B8 and B10 nanoparticles, no growth of *A. flavus* was observed at 10 mg. The PI of B6, B8 and B10 nanoparticles increased with amount of silver@silica nanoparticle. But, as expected, B6 (8% Ag) nanoparticles had significantly lower percent inhibition ($P < 0.05$) than those of B8 (9% Ag) and B10 (11% Ag) nanoparticles. B8 and B10 nanoparticles had PI that were not significantly different ($P > 0.05$), reaching 100% at 10 mg.

Effect of ammonia

Ammonia was used in the synthesis of Silver @ Silica nanoparticles as a catalyst for condensation hydrolysis reaction of alkoxysilane precursors (TEOS and APTES) which leads to the formation of the silica layer. However, hydroxide groups (OH-) that ammonia provides during this catalysis can be provided by APTES which has an amine group. Thus, to avoid the formation of [Ag (NH 3) 2] + (aq) which would reduce the amount of encapsulated silver, silver@silica type B8 nanoparticles were synthesized under the same conditions but without addition of ammonia in the reaction medium. The nanoparticles obtained were presented on the TEM images of **Figure 5**.

The nanoparticles observed on TEM images were mainly core-shell structures despite the absence of ammonia. In addition, amount of silver encapsulated by nanoparticles was greater compared to that obtained during the synthesis with ammonia. However, there were unencapsulated silver nanoparticles and less defined silver@silica forms. The results obtained after size measurements were presented in **Table 5**.

B8 nanoparticles synthesized without ammonia completely inhibited growth *A. flavus* at 10 mg. Their antifungal activity was similar to that of B8 nanoparticles synthesized with ammonia (**Table 6**). Statistical analyzes showed that there was no significant difference between PI of B8 nanoparticles and those B8 synthesized without ammonia.

Tableau 1. Characteristics of B4 nanoparticles

Type	Diameter of silver (nm)	Diameter of silica (nm)	Silver weight %
B4	2-10	60-78	6

` Tableau 2. Antimicrobial activity versus B4 nanoparticles quantity.

Quantity (mg)	PI of B4 nanoparticles
2	16 ± 1.2
4	27 ± 5.4
8	61 ± 3.2
20	72 ± 4.5
30	100 ± 0.0

Tableau 3. Characteristics of B6, B8 and B10 nanoparticles

Type	Diameter of silver (nm)	Diameter of silica (nm)	Silver weight %
B6	2-9	30-91	8%
B8	2-12	29-109	9%
B10	2-8	35-98	11%

Table 4. Antimicrobial activity versus B6, B8 and B10 nanoparticles quantity.

Quantity of nanoparticles (mg)	PI of B6 nanoparticles	PI of B8 nanoparticles	PI of B10 nanoparticles
4	53 ± 2.3^{a}	73 ± 3.5^{b}	71 ± 2.3^{b}
6	66 ± 4.7^{a}	88 ± 6.6^{b}	83 ± 5.7^{b}
8	76 ± 4.5^{a}	93 ± 4.7^{b}	93 ± 4.7^{b}
10	92 ± 3.2^{a}	100 ± 0.0^{b}	100 ± 0.0^{b}

Means followed by the same lowercase letter in each line are not significantly different using Tukey-Kramer test at $p < 0.05$

Tableau 5. Characteristics of B8 nanoparticles synthesized without ammonia

Type	Diameter of silver (nm)	Diameter of silica (nm)
B8	2-10	20-91

Tableau 6. Antimicrobial activity versus of B8 nanoparticles and B8 nanoparticles without NH_4OH

Quantity of nanoparticles (mg)	PI of B8 nanoparticles	PI of B8 nanoparticles without NH_4OH
4	73 ± 3.5[a]	75 ± 4.5[a]
6	88 ± 6.6[a]	89 ± 2.3[a]
8	93 ± 4.7[a]	96 ± 3.7b[a]
10	100 ± 0.0[a]	100 ± 0.0[a]

Means followed by the same lowercase letter in each line are not significantly different using Tukey-Kramer test at $p < 0.05$

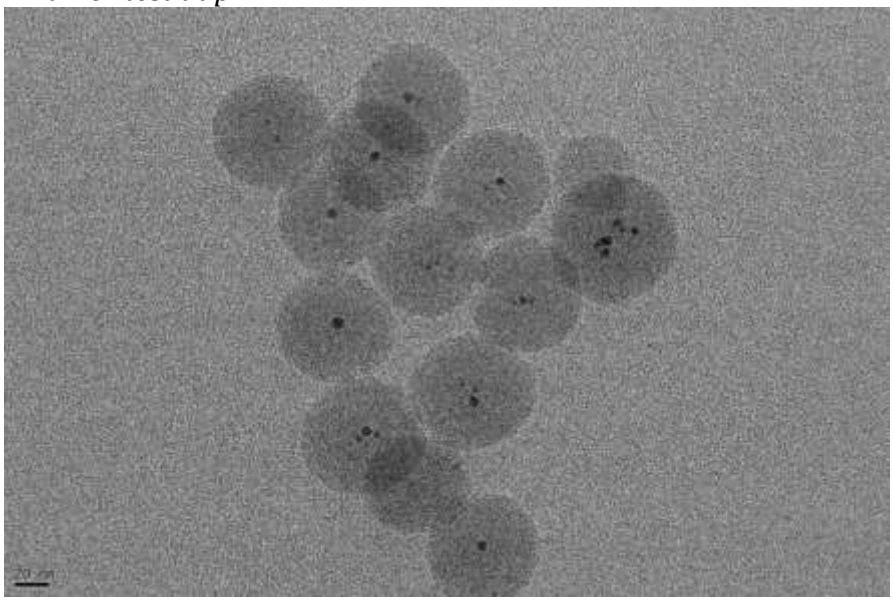

Figure 1. Transmission electron microscopy image of silver@silica type B4 nanoparticles

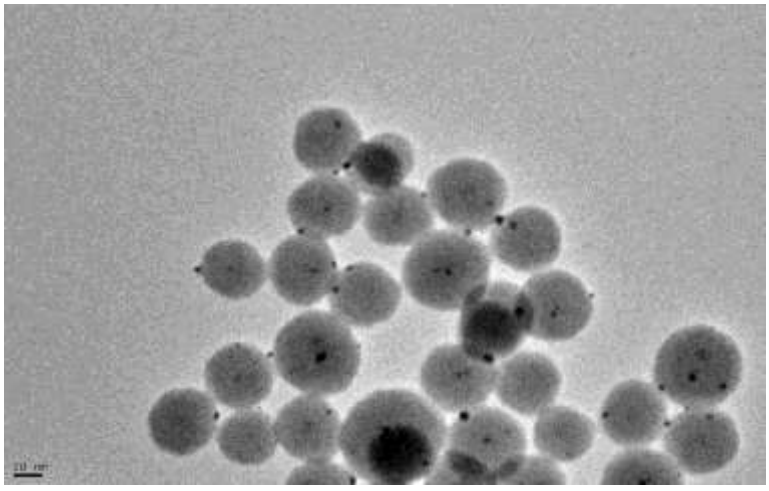

Figure 2. Transmission electron microscopy images of silver@silica type B8 nanoparticles (with 8g/L of silver in the aqueous phase of the microemulsion)

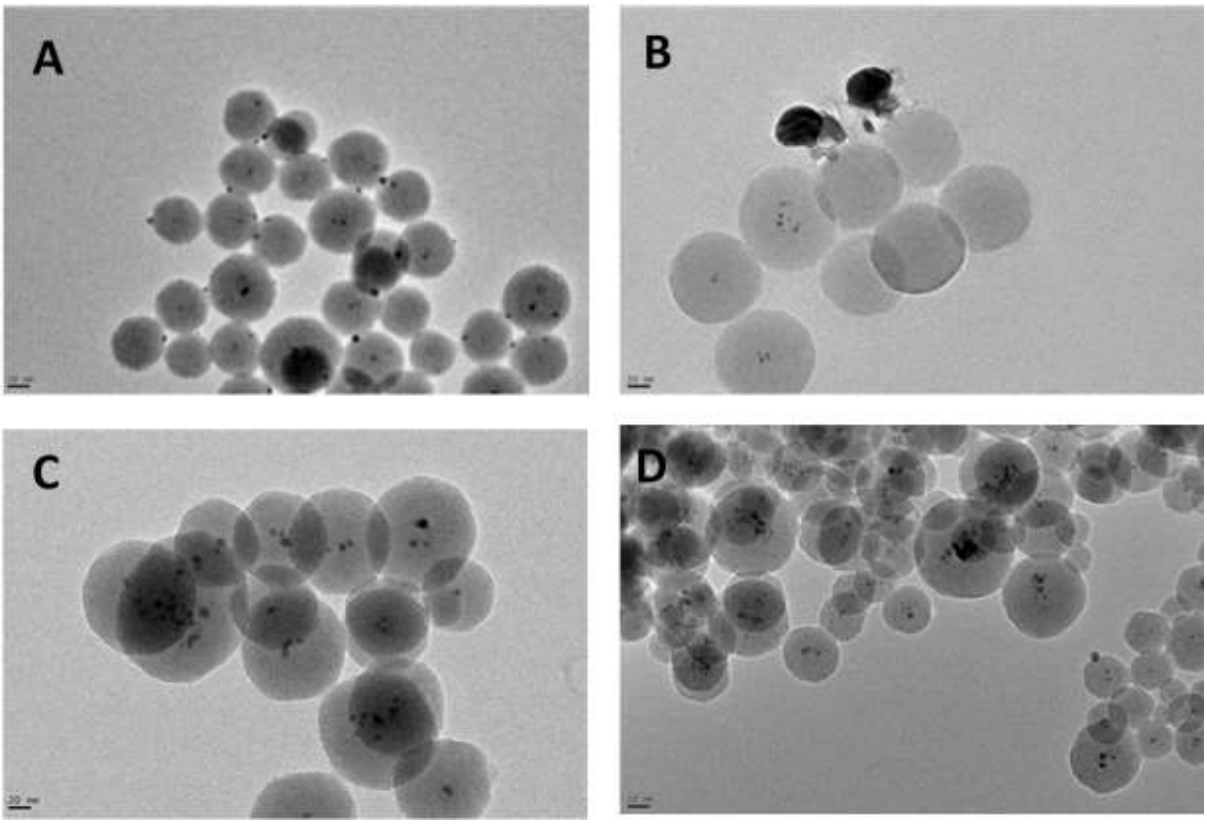

Figure 3. Transmission electron microscopy images of B8 nanoparticles. Variation of %APTES: A (20%), B (30%), C (35%), D (40%)

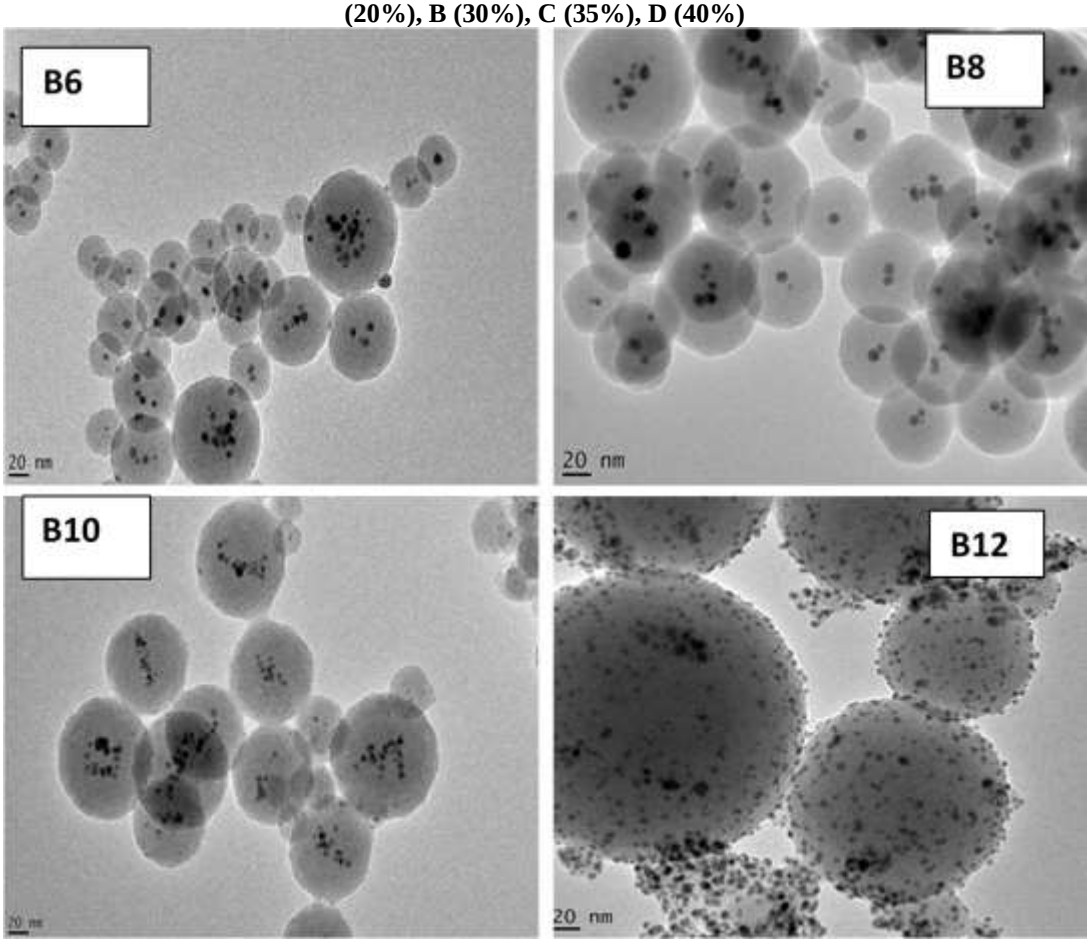

Figure 4. Transmission electron microscopy images of B6, B8, B10 et B12 nanoparticles synthesized with mass concentrations of 6, 8, 10 and 12g/L Ag+ in the aqueous phase of microemulsion, respectively.

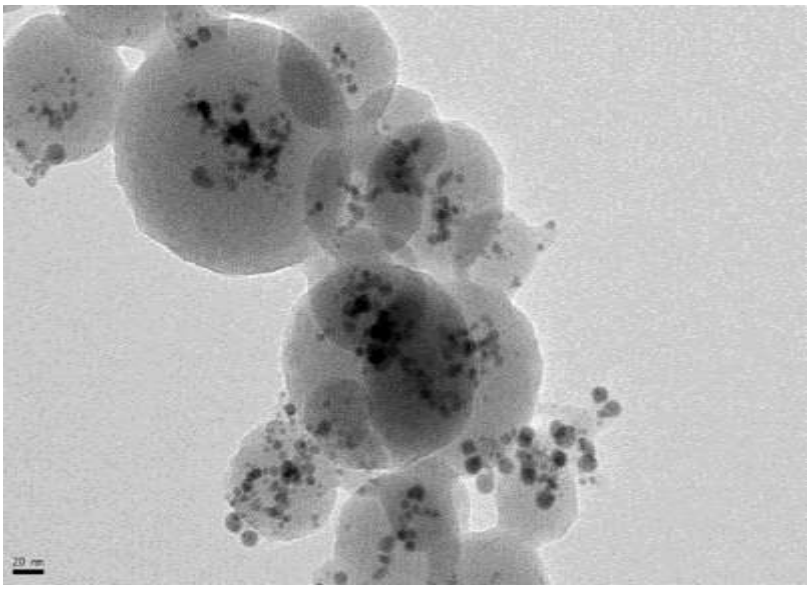

Figure 5. MET images of silver@silica B8 nanoparticles synthesized without addition of ammonia in the reaction medium

DISCUSSION

The antimicrobial action of silver@silica nanoparticles against *Aspergillus flavus* depends on the percentage of silver encapsulated in the silica matrix. There was an increase in the antimicrobial character of silver@silica nanoparticles as the percentage of silver encapsulated in the silica matrix increased. This result was observed by Diop **[4]** on strains of bacteria. Indeed, the increase in the amount of silver in the microemulsion led to an increase in nanometric silver encapsulated in silica nanoparticles, which in turn increased the antimicrobial efficacy of silver@silica nanoparticles. Thus, after optimization of silver@silica nanoparticles, the minimum inhibitory concentration which was 30 mg per box for B4 nanoparticles (6% Ag) was divided by three by passing to nanoparticles B8 which contains 9% of silver. The antimicrobial effect of silver@silica nanoparticles can therefore be controlled by the variation of the percentage of silver encapsulated in the silica matrix. However, the antimicrobial efficacy was almost similar between the nanoparticles B8 (9% Ag) and B10 (11% Ag) on *Aspergillus flavus*. These results demonstrate the existence of an optimum of inhibition when the percentage of encapsulated silver is equal to 9%. Moreover, beyond 10 mg/L of silver solubilized in the microemulsion, silver nanoparticles began to be found gradually outside the silica shell until the loss of core@shell structure. Thus, there is also a threshold concentration of silver in the

microemulsion beyond which the silver nanoparticles are no longer encapsulated in the silica matrix. In our synthesis conditions this threshold concentration was 10 mg/L.

Silver@silica nanoparticles have greater antimicrobial activity compared to naked silver nanoparticles **[7]**. This result is attributed to the silica shell which limits the uncontrolled dissolution of the encapsulated silver resulting in a prolonged release of the silver ions through the porous silica shell. Silver nanoparticles that are not protected by silica have limited use. In fact, their low colloidal stability as well as the adsorption on their surface of the intracellular substances of the dead microbes can prevent them from continuing to release Ag+ ions in the medium and thus alter their sustainable biocidal activity **[8]**. It is therefore particularly interesting to cover them with a layer of silica capable of protecting them.

CONCLUSION

Silver@silica hybrid nanoparticles with a well-defined core@shell structure were synthesized by reverse microemulsion. Tests carried out showed that silver@silica nanoparticles had a very good antimicrobial activity against Aspergillus flavus. Detailed examination of synthesis parameters that influence antimicrobial character of silver@silica nanoparticles allowed us to design an antimicrobial agent with an optimal cost/efficiency ratio with an oligodynamic character.

REFERENCE

1. Bhattacharya R, Mukherjee P (2008) Biological properties of “naked” metal nanoparticles. Adv Drug Deliv Rev 60:1289-1306.

2. Gaffet E. (2009) Nano Argent/Nano Silver. Nanomaterials Research Group-CNRS-Belfort. Avril 2009, 91p.

3. Egger S, Lehmann R P, Height M J, Loessner M J, Schuppler M (2009) Antimicrobial Properties of a Novel Silver-Silica Nanocomposite Material. Appl Environ Microbiol 75:2973-2976.

4. Diop BN (2010) Elaboration de nanoparticules hybrides multifonctionnelles à base de silice par microémulsion inverse Application à la conception d’un agent antibactérien. Thèse de doctorat de 3ème Cycle de Chimie. Université Claude Bernard Lyon 1, 159p.

5. Zheng LP, Zhang Z, Zhang B, Wang JW (2012) Antifungal properties of Ag-SiO2 core-shell nanoparticles against phytopathogenic fungi. Adv Mater Res 476:814-818.

6. Knopp D, Tang D, Niessner R. Review: bioanalytical applications of biomolecule-functionalized nanometer-sized doped silica particles (2009) Anal Chim Acta 1:14-30.

7. Acharya D, Mohanta B, Pandey P (2018) Antibacterial Properties of Synthesized Ag and Argent@Silice Core-Shell Nanoparticles: A Comparative Study. Can J Phys 8:955-960.

8. Kong H, Jang J (2008) Antibacterial Properties of Novel Poly(methylmethacrylate) Nanofiber Containing Silver Nanoparticles. Langmuir 24:2051-2056.